Spatial inhomogeneity of impact-ionization switching process in power Si diode

© S.K. Lyubutin[1], V.E. Patrakov[1,2], S.N. Rukin[1], B.G. Slovikovsky[1], S.N. Tsyranov[1]

[1] Institute of Electrophysics Ural Branch of Russian Academy of Sciences,
620016 Yekaterinburg, Russia
[2] Ural Federal University,
620002 Yekaterinburg, Russia

E-mail: ganimed323@mail.ru

Received April 17, 2023
Revised July 3, 2023
Accepted October 2, 2023

Voltage drop process in power Si diode switched to a conducting state by an impact-ionization wave, which is excited by overvoltage pulse with a subnanosecond rise time, has been investigated. In experiments, a reverse voltage pulse was applied to a diode with a diameter of 6 mm without preliminary reverse bias, which provided the average rate of voltage rise across the diode dU/dt in the range of $1-10$ kV/ns. Numerical simulations showed that calculated and experimentally observed voltage waveforms are in good quantitative agreement in the case when an active area of the structure S_a, through which a switching current flows, increases with dU/dt value increasing. It was shown that at $dU/dt < 2$ kV/ns the active area tends to zero, and at $dU/dt > 10$ kV/ns it approaches the total area of the structure. Comparison with the results of similar studies shows that the increase in the active area of the structure with the increase in the S_a value does not depend on the material of the structure (silicon and gallium arsenide), the number of layers in the semiconductor structure (diodes and thyristors), and also on the value of the initial bias voltage.

Keywords: impact ionisation, voltage rise rate, active area, switching time.

DOI: 10.61011/SC.2023.07.57429.4871

1. Introduction

The discovery by Grekhov and Kardo-Syssoev of the effect of wave shock-ionization breakdown in a semiconductor diode [1] observed at a rapid (units of ns) rise of the reverse voltage led to the creation of a new class of powerful nano- and picosecond semiconductor switches (see the works [2–6,7] and references therein). Despite the large amount of research conducted, one of the fundamental issues of such a switching mechanism has not yet been unambiguously assessed, namely, the degree of heterogeneity of the switching process over the area of the structure. Research on this issue has been conducted before [8–12], and interest has increased markedly recently [13–16]. Under the assumption of current switching only over a part of the structure area, the question of the number and transverse size of local plasma formations or channels through which the device switching and further current flow occurs remains open. In application, the inhomogeneity degree of the current distribution over the area determines the voltage drop across the device and the energy loss in it.

The most significant factor determining the value of the active area of the S_a structure (the area through which the switching current flows) has been established. Such a factor is the rate of voltage rise on the structure dU/dt before its transition to the conducting state. Thus, in [8,9], visual observation of luminescence from GaAs diodes was carried out. In the work [8] at dU/dt in units of V/ns, current switching occurred along separate luminous channels, the number of which increased with the increase in the rate of voltage rise on the diode, and in the work [9] at dU/dt in tens of kV/ns, a homogeneous breakdown over the entire area of the diode without the formation of local channels was observed. In [10] work, the positive role of increasing the dU/dt parameter on the switching process of the Si diode was also observed.

In the last few years, the influence of the dU/dt parameter on the active area of the structure has been investigated by studying the switching process of power thyristors in the shock-ionization wave [17–21] regime. It was found that the growth of dU/dt in the range from $0.5-1$ to $5-6$ kV/ns reduces the time of thyristor transition to the conducting state to the value $200-300$ ps [17,19–21], increases the temperature of the semiconductor structure, at which the start of the shock-ionization wave is realized, from 110 to 180°C [20], and due to the increase of the active area reduces the energy losses in the thyristor in $1.5-3$ times when the subsequent discharge current of the capacitive accumulator is passed through it [18,21].

Usually, when researching and applying such a current switching mechanism in diodes and dinistors (thyristors), a bias voltage is applied to them in the reverse direction beforehand. For dinistors and thyristors, this voltage represents the charging voltage of the capacitive storage device. There is another less common mode of operation where there is no pre-shift on the instrument. In particular, semiconductor diode edge sharpeners embedded in the inner conductor break of a coaxial power transmission line operate in this mode [6,16,22]. When such diodes are

connected in series in a column, the switchable power reaches hundreds MW with edge durations of a few tens of picoseconds [23].

In the present work, the spatial heterogeneity of shock-ionization switching of a silicon power diode without prior reverse bias has been investigated at dU/dt values in the range 1−10 kV/ns.

2. Experimental

Scheme of the experiment is presented in Figure 1. An oscillator *1* with a semiconductor current breaker [24] was used to generate the reverse voltage pulses acting on the diode under study. When the pump capacitor C is charged, its charge current flows through the current interrupter diodes $SOS1$ and $SOS2$ in the forward direction. Then, after saturation of the magnetic key core MS, reverse current is injected into the diodes, and the capacitor energy is transferred to the inductive storage L and the inductance of the back-pumping circuit. When the reverse current is interrupted at the generator output (transmitting coaxial line L, outer diameter 30 mm, wave impedance 48 Ohm) a pulse with amplitude up to 100 kV and front ∼ 2 ns is formed. After the edge is sharpened by the sharpening agent SS, the amplitude of the pulse acting on the diode under study D in the absence of the resistor R is ∼ 75 kV with an edge of 400 ps. The generator and transmission line are filled with transformer oil.

The operating conditions of the diode under study D in the circuit of Figure 1 correspond to the mode of the pulse sharper, when its switching to the conducting state sharpen the front of the incident wave. In this case, there is no increase in the incident wave current. The wave effects of a diode installed in a coaxial path are described in more detail in [25]. In our case, the differences from the [24] conditions are as follows. Firstly, the amplitude of the incident wave is significantly higher (75 kV in our case and ∼ 1.5 kV in [25]). Secondly, the diode is installed not in the middle of the path, but at its end, which leads to the realization of a short-circuit mode of the transmission line when the diode is switched on.

The investigated power rectifier diode D was made by diffusion technology from B40 grade silicon with resistivity n-of silicon in the range 25−45 ohm · cm. The $p^+-p-n-n^+$-type structure had a thickness of 350 μm and a depth of the $p-n$-junction of 136 μm. Diode diameter — 6 mm, steady-state avalanche breakdown voltage U_b, measured at room temperature, — 1750 V.

The voltage from the diode D was directly fed into the 50-ohm signal recording path, which included a 3 m long cable with an cutoff frequency of > 18 GHz and high-voltage attenuators from „Barth Electronics“ with a bandwidth of 30 GHz. A Tektronix TDS-6154C real-time digital oscilloscope (bandwidth — 15 GHz, sampling — 25 ps) was used as a recorder. To reduce signal distortion due to the finite inductance of the diode connection to the measurement path, the diode under study was soldered directly to the measurement cable.

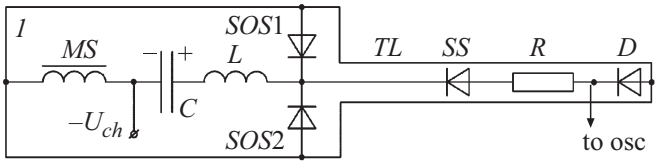

Figure 1. Scheme of the experiment (explanations in the text).

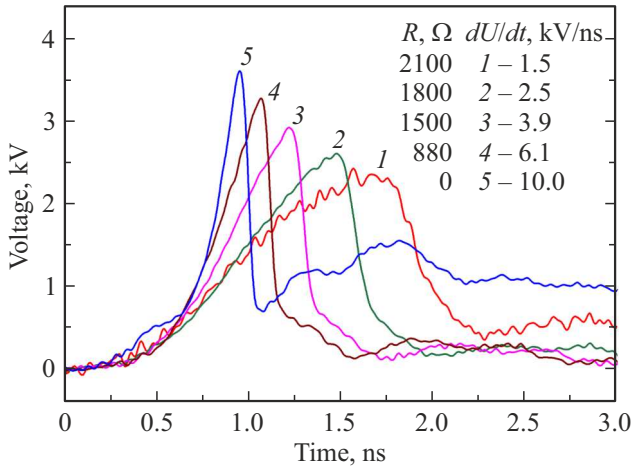

Figure 2. Oscillograms of the diode voltage during switching at different values of dU/dt (different values of resistor resistance R). (The colored version of the figure is available on-line).

The rate of voltage rise dU/dt on the diode was varied by changing the value of the resistance of the resistor R of the brand TVO-5 in the range from 0 (no resistor in the line) to 2 kOhm. The value of dU/dt was in the range 1−10 kV/ns and was estimated from the ratio $dU/dt = \Delta U/t_r$, where ΔU — the voltage drop across the diode between levels 0.1−0.9 from the amplitude value U_m, and t_r — the voltage rise time corresponding to this drop. The time 0.1−0.9, but the voltage drop was taken from the value U_m to the beginning of the slow part of the voltage drop corresponding to the residual voltage across the diode. Each experimental point (oscillogram) at a fixed value of resistance R was obtained by averaging 10 consecutive oscillograms.

Characteristic oscillograms of voltage pulses on the diode at different values of dU/dt are shown in Figure 2, and the results of processing oscillograms — in Figure 3. For convenience, the voltage, current, and electric field strength in the figures in this article are given in positive polarity. It can be seen that increasing the voltage rise rate from 1 to 10 kV/ns significantly changes the diode switching characteristics: the switching voltage U_m increases 1.7 times, the voltage rise time t_r decreases 4.5 times, and the diode transition time to the conducting state t_s decreases 9 times, reaching a value of 48 ps.

The above non-standard way of estimating the diode switching time — from the value of U_m to the beginning of the slow voltage decay section — is due to the existence of residual voltage on the diode after it has switched. This

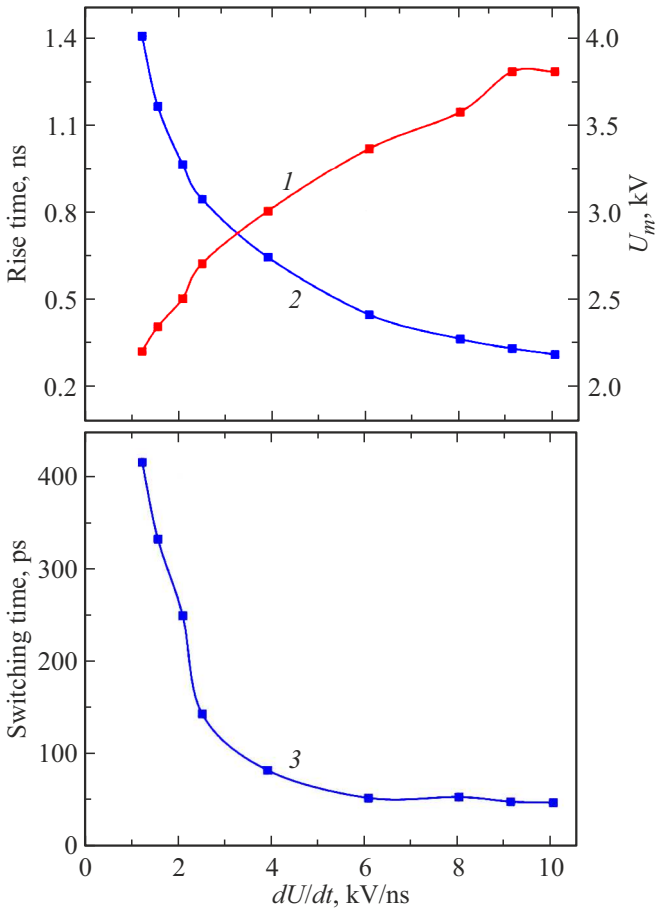

Figure 3. Experimental dependences of the maximum diode voltage (*1*), voltage rise time (*2*) and switching time (*3*) on the diode voltage rise rate.

is due to the fact that after the shock-ionization wave has passed through the diode, narrow regions with high electric field remain in the diode structure. This will be shown further (see Figure 7 in the theoretical part of the work).

It is also necessary to note the peculiar behavior of the residual voltage curve in the variant with the maximum value of dU/dt (10 kV/ns, curve *5* in Figure 2). Here, the residual voltage does not decrease with time, but instead increases after the diode switches to the conducting state. This behavior of the voltage curve is due to the implementation of the short-circuit mode of the transmission line and an increase in the current through the diode, since the resistor R is absent in the circuit.

3. Calculation part

3.1. Model description

The calculations were carried out using a model consisting in the joint solution of the telegraph equations for the line including the diode and the equations describing the dynamics of carriers, electric field and temperature in the diode structure. The continuity equations are used for carrier dynamics, and the Poisson equation is used for the electric field. Carrier velocity dependences on electric field, temperature, scattering on impurities and electron-hole scattering are used. The processes of avalanche multiplication, tunneling carrier generation, and ionization of deep impurities are taken into account. A detailed description of the model is given in [26].

In calculation, the real distribution of impurities in the structure of the diode under study is taken into account. The diodes have an $p^+-p-n-n^+$-type structure with a thickness of 350 μm and a diameter of 6 mm with impurities distributed as follows: p^+-band is formed by boron diffusion (10^{19} cm^{-3}, 80 μm), p-band — aluminium diffusion (10^{17} cm^{-3}, 136 μm), n^+-band — phosphorus diffusion (10^{19} cm^{-3}, 60 μm). The numbers in brackets correspond to the impurity concentration at the boundary and its depth of occurrence. The diode is made of n-type silicon with a resistivity of $\rho = 20-45$ Ohm $\cdot$ cm.

The calculations were performed under the assumption that avalanche propagation is triggered once the carrier concentration exceeds the n_0 [27] value. This condition is widely used to prevent the switching process from being affected by avalanche propagation of unphysically small carrier concentrations [17,19,26,29].

As was shown in [29], deep levels of the M type with energy 0.54 eV can have a significant influence on the switching process. The issue of NPI concentration of such deep levels in silicon structures is currently not completely clarified. In [28] it was shown that the value of N_{PI} lies within a wide range of $10^{11}-10^{13}$ cm^{-3}. On the other hand, a recent work [30] found that p^+-n-n^+-type structures do not have such deep levels, but $p^+-p-n-n^+$-type structures do. In the present work, $N_{PI} = 10^{12}$ cm^{-3} and $n_0 = 0.5 \cdot 10^9$ cm^{-3} are adopted, providing the best agreement between computational and experimental data in [17]. Since the voltage pulse was applied to the structure without prior reverse bias, i.e., filled with basic carriers, the influence of the concentration of deep impurities N_{PI} and the value of n_0 on the calculation results is small.

During the calculations, the condition that after the onset of shock-ionization processes, the structure is divided into an active part, where ionization processes occur, and a passive part, where ionization processes do not occur, is accepted. We introduce the parameter $K = S/S_a$, which is equal to the ratio of the total and active area [13]. Assuming that the shock-ionization front is flat, and the current is uniformly distributed over the area, we use the one-dimensional approximation to model the carrier dynamics in the active and passive parts of the diode. It is accepted that the separation of the structure into active and passive parts occurs when the field strength reaches the ionization threshold at any point of the structure:

$$E > E_b, \tag{1}$$

where $E_b = 1.8 \cdot 10^5$ V/cm — the electric field value corresponding to the ionization threshold in silicon. Note that changing the value of E_b in the range from 0 to $2 \cdot 10^5$ V/cm does not affect the calculation results.

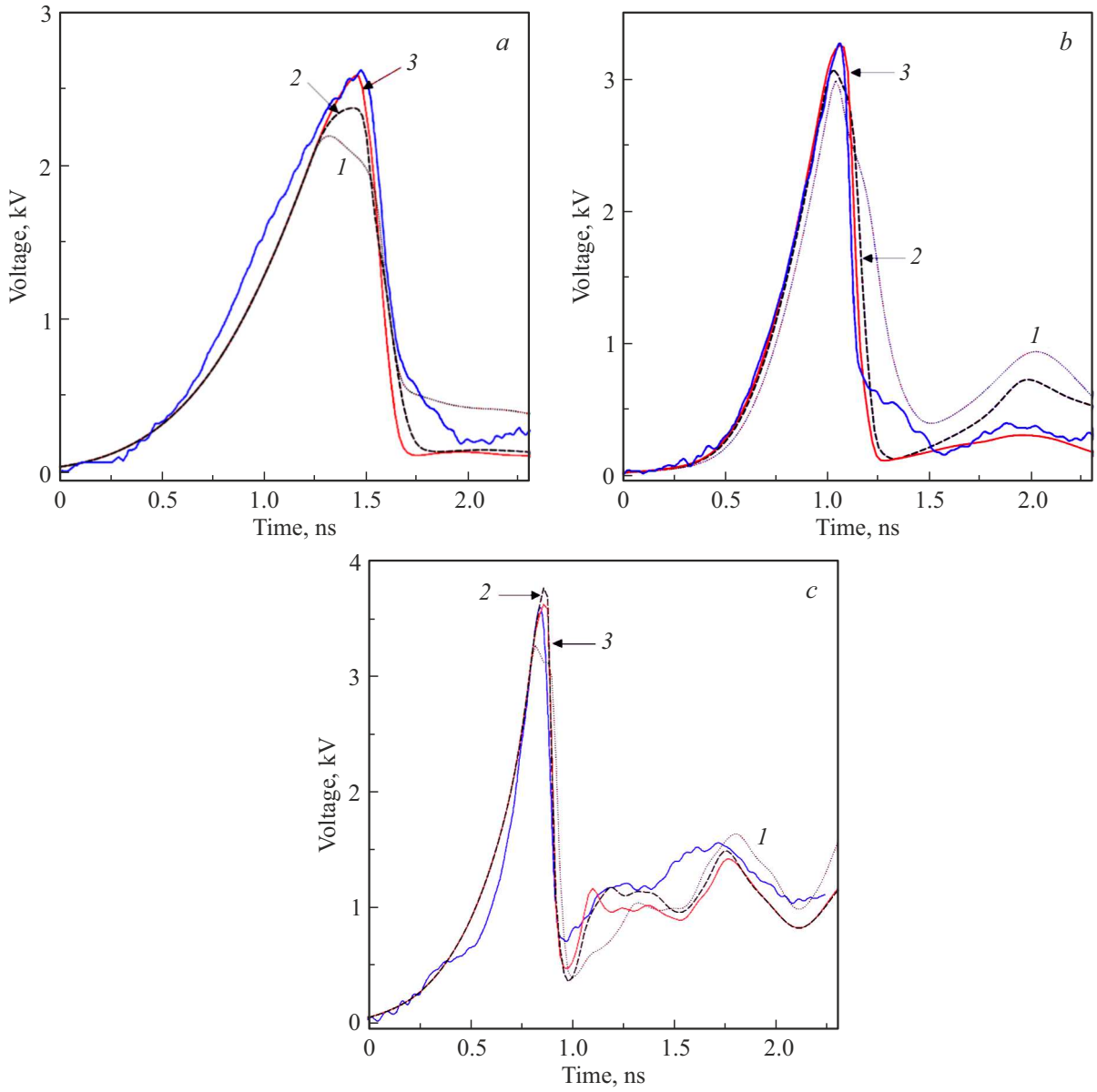

Figure 4. Comparison of experimental (solid blue curve) and calculated voltage versus time relationships for three values of the coefficient K (curves *1–3*): *a* — $dU/dt = 2.5$ kV/ns at $K = 3$, 6, 12; *b* — $dU/dt = 6.1$ kV/ns at $K = 1.1$, 2, 4; *c* — $dU/dt = 10.0$ kV/ns at $K = 1.1$, 3, 2.7. The *3* curve is closest to the experimental one. (The colored version of the figure is available on-line).

The operation of the experimental electrical circuit in the calculation is given by telegraphic equations. For a detailed description, see [23].

3.2. Dependence of active area on the rate of voltage rise

In calculations, voltage pulses with values dU/dt, close to the experimental ones, were applied to the diode under study (see Figure 2). The $K = S/S_a$ parameter in the calculations ranged from 1.2 to 30. The results of calculations in comparison with the experiment are shown in Figure 4. Results are presented for three of the experimental oscillograms shown in Figure 2. For each oscillogram, three calculated dependencies are shown for different K, where the one closest to experiment is shown under the number *3*.

Figure 5 shows the dependence of the value of K, which provides the best agreement with experiment (dark triangles), as a function of dU/dt. It can be concluded that the modelling adequately describes the experimental voltage dependences on the diode only when the value of the parameter K decreases with increasing dU/dt. It can also be seen that at $dU/dt < 2$ kV/ns the parameter K grows unboundedly, and at $dU/dt > 10$ kV/ns tends to 1. Since $K = S/S_a$, this corresponds to the fact that at $dU/dt < 2$ kV/ns the active area tends to zero and at $dU/dt > 10$ kV/ns approaches the total area of the

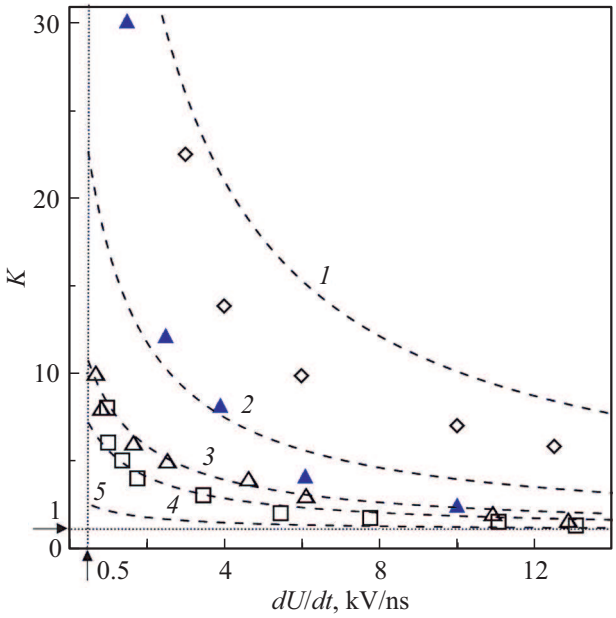

Figure 5. The dependence of the coefficient K on the voltage rise rate for a GaAs diode with a diameter of 0.3 mm and $\rho \sim 10\,\Omega\cdot$cm ($N_d \sim 6\cdot 10^{14}\,$cm^{-3}) (light rhombuses) [7], the silicon diode of 6 mm diameter investigated in this work with $\rho = 32\,\Omega\cdot$cm ($N_d \sim 1.5\cdot 10^{14}\,$cm^{-3}) (dark triangles), 40 mm diameter silicon thyristor with $\rho = 80\,\Omega\cdot$cm ($N_d \sim 0.6\cdot 10^{14}\,$cm^{-3}) (light triangles) [19], a 32-mm-diameter silicon thyristor with an $\rho = 105\,\Omega\cdot$cm ($N_d \sim 0.46\cdot 10^{14}\,$cm^{-3}) (light squares) [19]. The dotted curves *1–5* are plotted using the formula (2) for $\rho \sim 10$, 32, 80, 105, and 150 $\Omega\cdot$cm, respectively.

structure. The obtained result correlates with experimental observations of the extinction of the fast switching process at $dU/dt < 0.5\,$kV/ns [17]. In [19], data on the switching process of silicon thyristors were processed and a nonlinear approximation of the parameter K as a function of the base doping level and the value of dU/dt was found. The formula refined in the present work has the form

$$K = 1 + \frac{a}{dU/dt + 1}, \qquad (2)$$

where $a = 100 - 19.5\cdot\ln(\rho)$, dU/dt has the dimension kV/ns, ρ — silicon resistivity $\Omega\cdot$cm. Figure 5 shows the dashed curves plotted by formula (2) for silicon structures with resistivity $\rho = 32$, 80 and 105 $\Omega\cdot$cm (curves *2, 3* and *4*, respectively). The curves *3* and *4* describe well the dependences of the coefficient K on dU/dt obtained in [19] for silicon thyristors when switching in the pre-back bias mode (light triangles and squares).

The results of the present work (dark triangles) agree worse with the curve *2* constructed by (2). Also, the threshold value dU/dt, below which the active area tends to zero, increases from 1 kV/ns for thyristors to 2 kV/ns for diodes in the present work. These differences may be due to the fact that the concentration of initial carriers triggering the switching process is higher in the case without prior reverse bias than with it. Increasing the concentration of initial carriers increases the number of locations where current channels forming the active area occur and increases the threshold value dU/dt, above which an active area is formed and a fast switching process exists.

Also Figure 5 shows the dependence of the coefficient K on dU/dt for the GaAs diode $p^+-p-n-n^+$ ($\rho = 10\,\Omega\cdot$cm) plotted from the data of [8]. Photographs of luminescent areas appearing on the chamfer during switching without prior reverse bias under a voltage pulse with $dU/dt = 3-12.5\,$kV/ns are presented in work. Knowing the diode structure diameter of 0.3 mm and assuming that the active area is equal to the luminescent area, we can estimate the value K. As can be seen from Figure 5, the dependence of K on dU/dt for GaAs is similar to that for silicon structures, but is much worse described by the approximation (2) (light rhombuses and curve *1*), which is a consequence of the difference of mobility and avalanche multiplication coefficients of carriers in silicon and GaAs.

Figure 5 shows that for the same values of dU/dt, the active area is found to be larger in the semiconductor structure with higher resistivity of the parent material. This can be attributed to the fact that as the resistance of the conductor material increases, the electric field distribution becomes more homogeneous, resulting in an increase in the size of the band occupied by avalanche propagation. And though the field amplitude decreases, the total number of places where current channels arise, constituting the active area, appears to increase.

Figure 5 shows the curve *5* for the structure with $\rho = 150\,\Omega\cdot$cm. It can be seen that almost the whole area of the structure is involved in the current transfer process at $dU/dt > 10\,$kV/ns. Note that this result correlates with the work [31], where it was shown that at $dU/dt = 10\,$kV/ns in a silicon diode with $\rho > 300\,\Omega\cdot$cm, a homogeneous switching regime is realized, during which avalanche multiplication processes occur simultaneously at each point of the device base.

In [16] the switching process of an p^+-n-n^+-type silicon diode ($\rho = 33.2\,\Omega\cdot$cm) with a pre-applied reverse bias under a voltage pulse with $dU/dt \sim 3\,$kV/ns was investigated. The calculation and experiment were compared at three values of $K = 1$, 4, 10. The best agreement is obtained at $K = 4$. Formula (4) gives for [16] twice the value of K. Note that in [16], the calculated pulse has 10% larger amplitude than the experimental pulse with good agreement in switching time. If the amplitude of the calculated pulse decreases and becomes closer to the experimental value, it is necessary to reduce the active area, i. e., increase K, possibly to 8, to preserve the switching time. The calculation using the model given in this work gives the best agreement with experiment [16] when the amplitude of the calculated pulse is 5% smaller than the experimental value and $K = 7$.

3.3. Switching process

Consider the switching process of an experimental diode with $\rho = 32\,\Omega\cdot$cm by a voltage pulse increasing at a

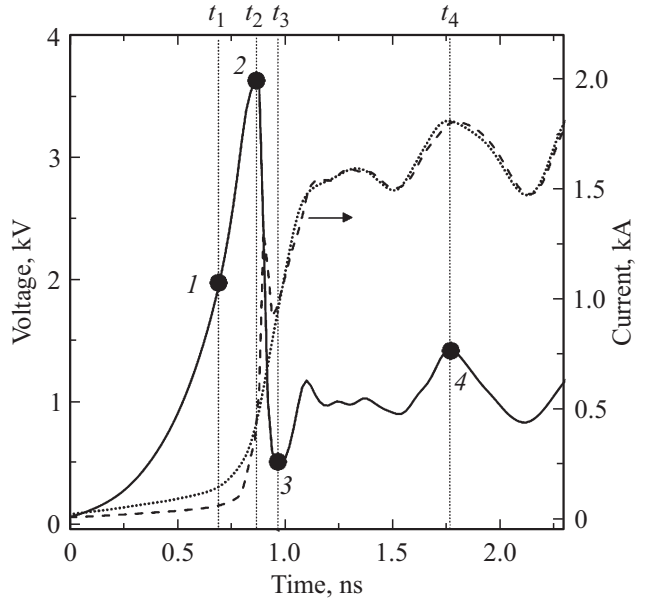

Figure 6. Calculated time-dependent voltage (solid curve) and current (dashed curve) across the active area of the diode at $K = 2.7$. The dot curve shows the current through the total area of the diode.

rate of $dU/dt \sim 10\,\text{kV/ns}$. A comparison of the calculated and experimental stress-time dependences is shown in Figure 4, *c*. It can be seen that the best agreement is obtained at $K = 2.7$. Let us consider the results of this calculation in more detail.

Figure 6 shows the stages of the switching process: the stage of field amplitude growth until the condition (1) is fulfilled and the diode is divided into active and passive parts, then the shock-ionization front is launched in the volume charge band of the SCB ($0-t_1$), the stage of filling the diode structure with plasma ($t_1 - t_2$), the switching stage ($t_2 - t_3$), and the stage of transition of the electron, hole and field distribution to the equilibrium state ($t > t_3$).

In the first ($0-t_1$) stage, when a rising voltage pulse is applied, electrons and holes are displaced in opposite directions from the $p-n$-junction plane, forming a space charged band (SCB). As the voltage increases, the concentration of carriers in the SCB decreases, the width of the SCB increases, and the size of the neutral part of the *n*-base decreases. Two bands with qualitatively different field distributions are formed in the diode structure: linearly increasing to a maximum in the plane of the $p-n$-junction in the SCB and homogeneous in the neutral part of the base (curve *1* in Figure 7).

By the time the condition (1) is fulfilled, the concentration of holes and electrons in the $p-n$-junction plane reaches $9.1 \cdot 10^{10}$ and $1.4 \cdot 10^{11}\,\text{cm}^{-3}$, respectively. The electron concentration is much less than the equilibrium concentration in the neutral part of the base ($N_d \sim 1.5 \cdot 10^{14}\,\text{cm}^{-3}$), but exceeds $n_0 = 0.5 \cdot 10^9\,\text{cm}^{-3}$ — the condition for triggering the avalanche propagation process in the model. The carrier concentration decreases as the width of the SCB increases, but at some point starts to increase due to the arrival of non-core holes and electrons from the *n*- and *p*-bands, respectively. The essential part of holes is formed due to shock-ionization processes in the neutral part of the *n*-base. This source of carrier input to SCB was first proposed in [32] and discussed in detail further, for example in [27]. At the voltage growth stage, the concentration of electrons and holes in the SCB is always much higher than the value of n_0 and the ionization processes start immediately upon reaching the electric field value necessary for this purpose.

Note that in the mode with pre-reverse bias [18], most of the stress is concentrated in the SCB, and the concentration of carriers in the $p-n$-junction plane by the time the condition (1) is fulfilled is smaller than in the present calculation. The large concentration of carriers in the $p-n$-junction plane seems to be the reason for the increased active area in the mode without pre-back bias relative to the mode with pre-back bias (dark triangles and curve *2* in Figure 5).

After the condition (1) is fulfilled in the calculation, the diode is divided into active and passive parts. Further, the shock-ionization wave with carrier saturation velocity $V_s \sim 10^7\,\text{cm/s}$ moves away from the $p-n$-junction. At moment of time, when the carrier concentration in the $p-n$-junction plane begins to exceed the doping level of the *n*-base, the electric field is shielded and a shock-ionization front is triggered.

In the second ($t_1 - t_2$) stage, the shock-ionization front moves away from the $p-n$-junction plane, filling the SCB with electron-hole plasma. Simultaneously, avalanche propagation processes occur at each point of the neutral *n*-base. Thus, there are two bands with fundamentally different ways of filling the structure with plasma: by means of a shock-ionization front propagating in the SCB, and uniformly at each point of the neutral *n*-base. By the time t_2, the diode voltage reaches a maximum of 3.6 kV, the sizes of the SCB and the neutral part of the *n*-base — 90 and 100 μm with the concentration of non-basic holes in them — $5 \cdot 10^{15}$ and $1.8 \cdot 10^{15}\,\text{cm}^{-3}$, respectively. The distribution of hole concentration and electric field for this time instant is shown by the curve *2* in Figure 7, *a*.

In the third (t_2-t_3) stage, the shock-ionization front continues to propagate in both directions from the $p-n$-junction. The front velocity is times the saturated velocity of the carriers 5–8 times the saturated velocity of the carriers V_s. The carrier concentration in the neutral part of the base grows in a homogeneous way, simultaneously at each of its points. In this case, the voltage in the active part of the diode decreases rapidly, which discharges the capacitance of the passive part of the diode. The current through the active part of the diode increases rapidly (dashed curve in Figure 6), accelerating the process of its filling with plasma. By moment t_3 *n*-, the base and low-alloy part of the *p*-band are filled with plasma with density $\sim 6 \cdot 10^{15}\,\text{cm}^{-3}$ (curve *3* in Figure 7, *b*).

In the final stage of ($t > t_3$), the magnitude of the current flowing through the device increases rapidly due

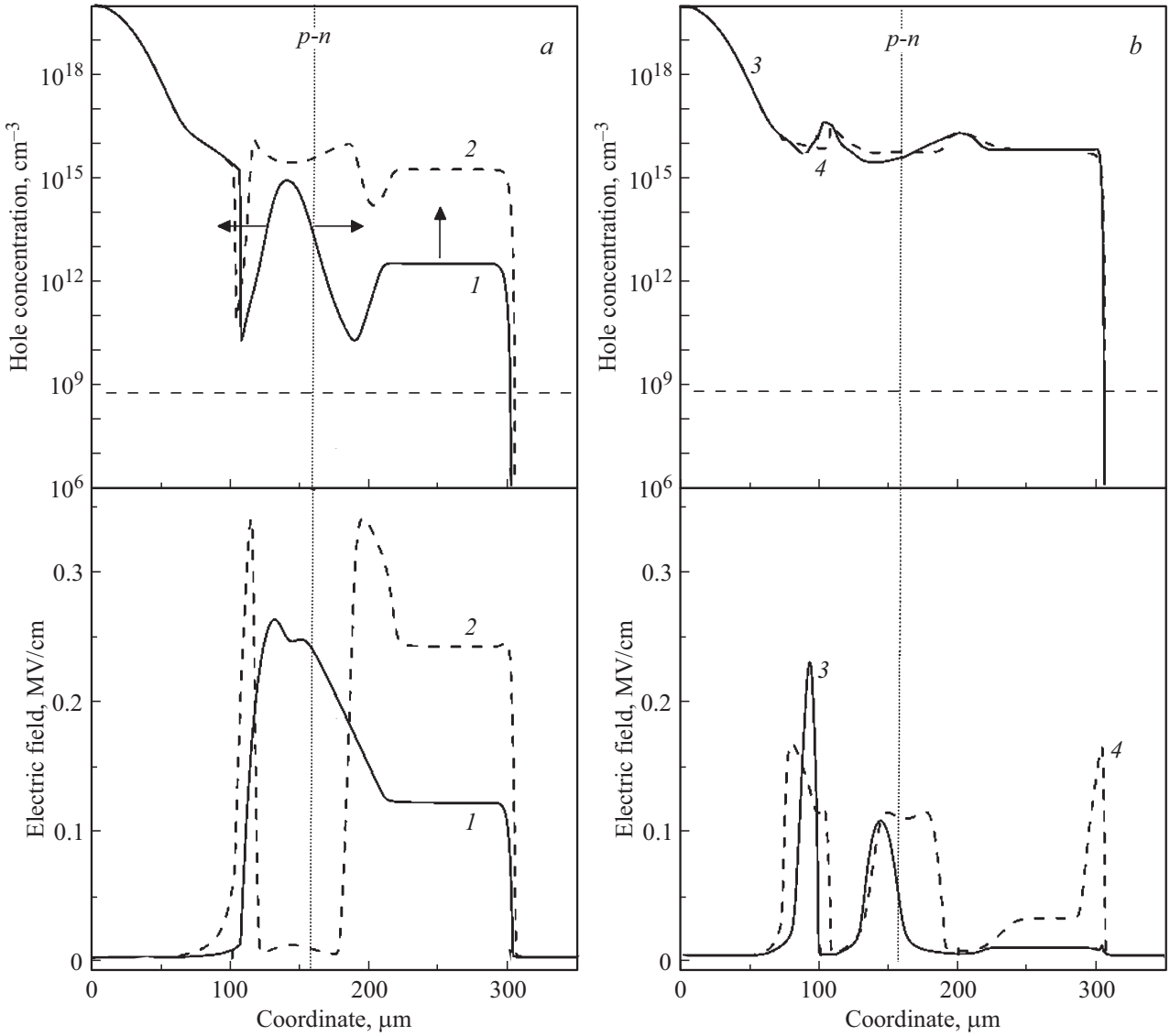

Figure 7. Profiles of the hole concentration distribution and electric field strength in the active part of the diode structure corresponding to the moments of time *1–4* in Figure 6. The arrows indicate the direction of motion of the ionization fronts.

to reflection from the shorted end of the line (dashed curve in Figure 6). In bands at the plasma boundaries and in the vicinity of the $p-n$-junction, where the concentration of carriers is relatively small, bands of strong field are formed (see the electric field curves *3* and *4* in Figure 7, *b*). Further, due to avalanche propagation processes, these bands are filled with additional carriers, as a result of which the field and voltage decrease. As the magnitude of the current remains large, carriers are continuously driven out of the plasma band, the field in the bands grows and the process repeats. In this case, the time dependence of the voltage becomes wavy (see the voltage curve in Figure 6).

4. Conclusion

A study of the switching process of a power diode by a voltage pulse increasing at a rate of up to 10 kV/ns has shown that the duration of the switching process is in the range of tens of picoseconds. Since there was no pre-applied reverse bias on the semiconductor structure, the voltage pulse was applied to the structure filled with basic carriers. In this case, there were two fundamentally different bands in the diode structure by the method of plasma filling: the band of the volume charge in the vicinity of the $p-n$-junction was filled by a shock-ionization wave moving at a velocity several times higher than the saturation velocity, and the band in the neutral part of the base was filled with plasma uniformly at each of its points (Figure 7, *a*). Ionization processes in SCBs are triggered by carriers, most of which appear due to the arrival of non-basic holes and electrons from the n- and p-bands, respectively. The essential part of holes is formed due to shock-ionization processes in the neutral part of the n-base. This source of carrier input to the SCB was first proposed in [32].

Despite the differences in the switching mechanism, the dependence of active area on dU/dt obtained for the diodes in this work correlates well with similar dependences obtained earlier for silicon thyristors [19] and GaAs diodes [8]. It is shown that with the growth of dU/dt the active area increases irrespective of the number of layers in the semiconductor structure (diodes and thyristors), the value of the voltage previously applied to the structure and the type of semiconductor (Si and GaAs). At $dU/dt < 1-2$ kV/ns the active area tends to zero, and at $dU/dt > 10$ kV/ns it approaches the full area of the structure. The obtained result is in agreement with the experimental observations of the extinction of the fast switching process in silicon thyristors at $dU/dt < 0.5$ kV/ns [17] and homogeneous breakdown over the whole area at dU/dt in tens of kV/ns in GaAs-diodes [9]. Note that at $dU/dt < 1$ kV/ns the shock-ionization front [3,7] is not formed in the structure, and the switching process proceeds, but much more slowly under the action of avalanche propagation waves moving with saturated velocity.

Apparently, the process of active area formation has a rather universal character. The number of places where current channels nucleate, constituting the active band, depends on the volume of the strong field band, the field amplitude and the number of carriers in it. With increasing dU/dt the size of the strong field band as well as the field amplitude in it, the active band increases accordingly. Naturally, the quantitative dependence of the active area on dU/dt is influenced by the mechanism of carrier formation triggering the switching process and the semiconductor material determining the mobility and avalanche multiplication coefficients of carriers. For example, as has been shown in the present work, while the dependence of the active area value on dU/dt is qualitatively the same, the functional approximation (2) for silicon and GaAs differs markedly from each other.

Funding

This study was carried out under partial financial support of the RSF grant No. 22-29-01257.

Conflict of interest

The authors declare that they have no conflict of interest.

References

[1] I.V. Grekhov, A.F. Kardo-Sysoev. Pisma v ZhTF, **5**, 950 (1979). (in Russian).
[2] A.F. Kardo-Sysoev. *New power semiconductor devices for generation of nano and subnanosecond pulses*, in *Ultra-Wideband Radar Technology*, ed. by J.D. Taylor (CRC Press, Boca Raton, 2001).
[3] M. Levinshtein, J. Kostamovaara, S. Vainshtein. *Breakdown Phenomena in Semiconductors and Semiconductor Devices* (World Scientific, London, 2005).
[4] I.V. Grekhov, S.V. Korotkov, P.V. Rodin. IEEE Trans. Plasma Sci., **36** (2), 378 (2008).
[5] I.V. Grekhov. IEEE Trans. Plasma Sci., **38** (5), 1118 (2010).
[6] V.I. Brylevskiy, I.A. Smirnova, A.V. Rozhkov, P.N. Brunkov, P.B. Rodin, I.V. Grekhov. IEEE Trans. Plasma Sci., **44** (10), 1941 (2016).
[7] B.C. DeLoach D.L. Sharfetter. IEEE Trans. Electron Dev., **17** (1), 9–21 (1970).
[8] S.N. Vainshtein, Yu.V. Zhilyaev, M.E. Levinshtein. Pis'ma ZhTF, **14** (16), 1526 (1988) (in Russian).
[9] I.V. Grekhov, V.M. Efanov. Pis'ma ZhTF, **16** (17), 9 (1990). (in Russian).
[10] A.F. Kardo-Sysoev, M.V. Popova. FTP, **30** (5), 803 (1996). (in Russian).
[11] A.M. Minarsky, P.B. Rodin. Solid-State Electron., **41** (6), 813 (1997).
[12] A.S. Kyuregyan. Pis'ma ZhTF, **31** (24), 11 (2005). (in Russian).
[13] P.B. Rodin, A.M. Minarsky, I.V. Grekhov. Pis'ma ZhTF, **38** (11), 78 (2012). (in Russian).
[14] M.S. Ivanov, N.I. Podolska, P.B. Rodin. J. Phys.: Conf. Ser., **816**, 012033 (2017).
[15] P.B. Rodin, M.S. Ivanov. J. Appl. Phys., **127**, 044504 (2020).
[16] M.S. Ivanov, V.I. Brylevskiy, I.A. Smirnova, P.B. Rodin. J. Appl. Phys., **131**, 014502 (2022).
[17] A.I. Gusev, S.K. Lubutin, S.N. Rukin, S.N. Tsyranov. FTP, **50** (3), 398 (2016).
[18] A.I. Gusev, S.K. Lubutin, S.N. Rukin, B.G. Slovikovsky, S.N. Tsyranov. PTE, **4**, 95 (2017). (in Russian).
[19] A.I. Gusev, S.K. Lubutin, S.N. Rukin, S.N. Tsyranov. FTP, **51** (5), 680 (2017). (in Russian).
[20] A. Gusev, S. Lyubutin, S. Rukin, B. Slovikovsky, S. Tsyranov, O. Perminova. Semicond. Sci. Technol., **33**, 115012 (2018).
[21] A.I. Gusev, S.K. Lyubutin, V.E. Patrakov, S.N. Rukin, B.G. Slovikovsky, M.J. Barnes, T. Kramer, V. Senaj. J. Instrumentation, **14** (10), 10006 (2019).
[22] A.S. Kesar, A. Raizman, G. Atar, S. Zoran, S. Gleizer, Y. Krasik, D. Cohen-Elias. Appl. Phys. Lett., **117**, 013501 (2020).
[23] A.I. Gusev, S.K. Lubutin, S.N. Rukin, B.G. Slovikovsky, S.N. Tsyranov. FTP, **48** (8), 1095 (2014). (in Russian).
[24] S.N. Rukin. Rev. Sci. Instrum., **91**, 011501 (2020).
[25] M.S. Ivanov, V.I. Brylevskii, P.B. Rodin. Pis'ma ZhTF, **47** (13), 32 (2021). (in Russian).
[26] S.K. Lyubutin, S.N. Rukin, B.G. Slovikovsky, S.N. Tsyranov. FTP, **46** (4), 535 (2012). (in Russian).
[27] P. Rodin, U. Ebert, W. Hundsdorfer, I.V. Grekhov. J. Appl. Phys., **92**, 1971 (2002).
[28]] E.V. Astrova, V.B. Voronkov, V.A. Kozlov, A.A. Lebedev. Semicond. Sci. Technol., **13**, 488 (1998).
[29] P. Rodin, A. Rodina, I. Grekhov. J. Appl. Phys., **98**, 094506 (2005).
[30] V.I. Brylevskiy, I.A. Smirnova, A.A. Gutkin, P.N. Brunkov, P.B. Rodin, I.V. Grekhov. J. Appl. Phys., **122** (18), 185701 (2017).
[31] S.N. Tsyranov, S.N. Rukin. *Proc. 15th Int. Symp. High Current Electronics* (Tomsk, Russia, 2008) p. 288.
[32] I.V. Grekhov, A.F. Kardo-Sysoev, L.S. Kostina. Pis'ma ZhTF, **5**, 961 (1979). (in Russian).

Translated by Ego Translating